Weierstraß-Institut
für Angewandte Analysis und Stochastik

im Forschungsverbund Berlin e.V.

Preprint ISSN 0946 – 8633

Passive mode-locking with slow saturable absorber: a delay differential model

Andrei Vladimirov [1], Dmitry Turaev [2],

submitted: 19th July 2004

[1] Weierstrass Institute
for Applied Analysis
and Stochastics,
Mohrenstrasse 39
D - 10117 Berlin
Germany
E-Mail: vladimir@wias-berlin.de

[2] Ben Gurion University
P.O.B. 653
84105 Beer-Sheva
Israel
E-Mail: turaev@cs.bgu.ac.il

No. 947
Berlin 2004

2000 *Mathematics Subject Classification.* 78A60,34C23.

Key words and phrases. semiconductor laser, mode-locking, delay differential equations, bifurcations.

1999 *Physics and Astronomy Classification Scheme.* 42.60.Fc,42.55.Px,42.60.Mi,42.65.Pc,42.60.Gd.

Edited by
Weierstraß-Institut für Angewandte Analysis und Stochastik (WIAS)
Mohrenstraße 39
10117 Berlin
Germany

Fax: + 49 30 2044975
E-Mail: preprint@wias-berlin.de
World Wide Web: http://www.wias-berlin.de/

Abstract

We propose and study a new model describing passive mode-locking in a semiconductor laser – a set of differential equations with time delay. Analytical analysis of this model is performed under the slow saturable absorber approximation. Bifurcations responsible for the appearance and break-up of mode-locking regime are studied numerically.

Passive mode-locking (ML) is a very powerful method to generate high quality short pulses with high repetition rates from different kinds of lasers. In particular, monolithic passively and hybrid mode-locked semiconductor lasers are compact, low cost, reliable, and efficient sources of picosecond and subpicosecond pulses ideal for applications in high speed communication systems [1]. Due to their small size, large gain coefficient and fast recovery time of semiconductor material these lasers can produce pulses at very high repetition rates (tens and hundreds of GHz). The duration of ML pulses generated by semiconductor lasers is typically much smaller than semiconductor saturable absorber recovery time. This situation is usually referred to as a ML with slow saturable absorber [2]. The basic physical mechanism responsible for the appearance of passive ML in a laser with slow absorber is well known [3]: Absorbing medium saturates faster with the arrival of a pulse than the amplifying one, and, therefore, opens a short net gain window for the pulse amplification which is necessary to compensate cavity round trip losses; the net gain window is closed by gain saturation.

Analytical approaches to describe passive ML with slow saturable absorber were developed by New [3] and Haus [2]. Both of them considered a situation of small gain and loss per cavity round trip. They noticed that in the case of slow absorber when the relaxation times of amplifying and absorbing media are much larger than the pulse duration, time evolution of the ML solution can be split into two stages. The fast stage corresponds to a short time interval when the amplitude of a pulse is large. Since saturable gain and absorption evolve on time scales much larger than the pulse duration, the relaxation processes in intracavity media can be neglected at the fast stage. The slow stage corresponds to a time interval between two subsequent pulses when the laser intensity is close to zero. At this stage gain and absorption recover slowly to their unsaturated values. The slow stage can be described by linear ordinary differential equations that are easily integrated analytically. However, analytical solution for the fast stage can be obtained only after introducing some additional approximations. Specifically, New assumed that there is no spectral filtering in the cavity. This means that infinitely large number of laser modes lock in to form an infinitely short pulse. Gluing the solutions obtained for the two stages

and using the ML pulse background stability condition that requires the net gain be negative during the slow stage [3], New obtained implicit analytical expressions for the stability boundaries of the ML regime in the laser parameter space.

Unlike New's theory, the one developed by Haus is able to describe such important characteristics of ML solution as pulse shape, pulse duration, and deviation of the ML repetition period from the cold cavity round trip time. Haus included into consideration spectral filtering under parabolic approximation [2]. He showed that even in the limit of infinitely broad bandwidth of the spectral filtering element, background stability boundaries of ML pulses are different from those obtained using New's approach, in which spectral filtering is neglected from the very beginning. In order to get analytical description of the ML phenomenon, Haus assumed that the pulse power is small enough, so that the intracavity media are weakly saturated. Under this approximation he derived a closed analytical expression for the ML pulse shape in terms of hyperbolic secant. This result was found to be in a good agreement with the experimental data obtained with dye laser [4]. Since then different modifications of the Haus master equation have been derived and analyzed [5, 6, 7, 8, 9, 10, 11, 12, 13, 14, 15, 16, 17, 18, 19].

Despite of significant success of the Haus' model, its applicability to describe adequately real laser systems is questionable in the situations when the approximations underlying this model are not satisfied. In particular, typical solid state lasers with semiconductor saturable absorbers are operated under conditions of complete saturation [20], i.e. in a situation when Haus' model is not applicable. On the other hand, semiconductor ML lasers typically have very high gain and losses per cavity round trip. Therefore, the classical models by New and Haus, both assuming small gain and loss per cavity round trip, fail to describe adequately ML in these lasers. This is why approaches based on direct numerical simulations of spatially distributed models have been mainly used to study ML of semiconductor lasers (for a review see Ref. [18]). Although these approaches in principle allow to reproduce experimental data with quite good accuracy, they give only little insight into the physical mechanisms involved. The purpose of this paper is to study a new delay differential model that is able to describe ML in the parameter range typical of semiconductor lasers. When deriving this model we do not use small gain and loss, weak saturation, as well as infinite bandwidth approximation. The only essential assumption we adopt concerns a ring cavity geometry with unidirectional lasing. Being more general than the classical ML models our model remains simple enough to perform comprehensive bifurcation analysis and allows physical interpretation of the obtained results in terms similar to those used by New and Haus, such as, for example, the net gain parameter. Here we present a numerical study of the delay differential model and describe bifurcations responsible for the appearance and break-up of the ML regime. We show that under certain approximations analytical results obtained by New and Haus can be recovered from our model. Furthermore, we generalize their approaches to the case of large gain and loss per cavity round trip.

1 Model equations

Let us consider a ring laser shown in Fig. 1. It is assumed that one of the two counterpropagating waves in the laser cavity is suppressed so that the lasing is unidirectional. The laser consists of five sections. Let z be the coordinate along the cavity axis. The first, $z_1 < z < z_2$, and the fourth, $z_4 < z < z_5$, sections are passive. The second, $z_2 < z < z_3$, and the third section, $z_3 < z < z_4$, contain saturable absorber and gain medium, respectively. The last, fifth section, $z_5 < z < z_1 + L$, acts as a spectral filter that limits bandwidth of the laser radiation. Here L is the cavity length. Traveling wave equations [21, 22] governing evolution of the slow varying electric field envelope $E(t,z)$ in the gain and absorber sections can be written in the form

$$\frac{\partial E(t,z)}{\partial z} + \frac{1}{v}\frac{\partial E(t,z)}{\partial t} = \frac{\mathrm{g}_r \Gamma_r}{2}(1 - i\alpha_r)\left[N_r(t,z) - N_r^{tr}\right] E(t,z), \tag{1}$$

$$\frac{\partial N_r(t,z)}{\partial t} = J_r - \gamma_r N_r(t,z) - v\mathrm{g}_r \Gamma_r \left[N_r(t,z) - N_r^{tr}\right] |E(t,z)|^2. \tag{2}$$

Here the subscript $r = g$ $(r = q)$ corresponds to the gain (absorber) section. The variables $N_g(z,t)$ and $N_q(z,t)$ describe carrier densities in the gain and absorber sections, respectively. The parameters $N_{g,q}^{tr}$ are the carrier densities evaluated at transparency threshold. The parameter v is the light group velocity which is assumed to be constant and equal in all five sections. The parameters $\alpha_{g,q}$, $\mathrm{g}_{g,q}$, $\Gamma_{g,q}$, and $\gamma_{g,q} = 1/T_{g,q}$ are, respectively, linewidth enhancement factors, differential gains, transverse modal fill factors, and carrier density relaxation rates in the gain and absorber sections. The parameter J_g describes injection current in the gain section. For the absorber section we have $J_q = 0$.

Evolution of the electric field envelope $E(t,z)$ in the passive sections is governed by Eq. (1) with zero right hand side:

$$\frac{\partial E(t,z)}{\partial z} + \frac{1}{v}\frac{\partial E(t,z)}{\partial t} = 0. \tag{3}$$

The spectral filtering section is assumed to be negligibly thin, i.e., $z_1 + L \approx z_5$. Transformation of the electric field envelope by this section is given by the relation

$$\widehat{E}(\omega, z_1 + L) = \widehat{f}(\omega)\,\widehat{E}(\omega, z_5), \tag{4}$$

where $\widehat{E}(\omega, z_5)$ and $\widehat{E}(\omega, z_1 + L)$ are the Fourier transformations of $E(t, z_5)$ and $E(t, z_1 + L)$, respectively. The function $\widehat{f}(\omega)$ in Eq. (4) describes the lineshape of the bandwidth limiting element.

In a ring cavity the electric field envelope E obeys periodic boundary condition

$$E(t, z + L) = E(t, z). \tag{5}$$

After the coordinate change $(t,z) \to (\tau, \zeta)$, where $\tau = \gamma_q(t - z/v)$ is a retarded time divided by the absorber relaxation time and $\zeta = z\gamma_q/v$ is a normalized coordinate

along the cavity axis, Eqs. (1) and (2) for gain and absorber sections can be rewritten in the following adimensional form:

$$\frac{\partial A(\tau,z)}{\partial \zeta} = \frac{1}{2}(1-i\alpha_g)\, n_g(\tau,z)\, A(\tau,z), \tag{6}$$

$$\frac{\partial n_g(\tau,z)}{\partial \tau} = j_g - \Gamma n_g(\tau,z) - n_g(\tau,z)\,|A(\tau,z)|^2, \tag{7}$$

$$\frac{\partial A(\tau,z)}{\partial \zeta} = -\frac{1}{2}(1-i\alpha_q)\, n_q(\tau,z)\, A(\tau,z), \tag{8}$$

$$\frac{\partial n_q(\tau,z)}{\partial \tau} = -j_q - n_q(\tau,z) - s n_q(\tau,z)\,|A(\tau,z)|^2. \tag{9}$$

Here $A(\tau,\zeta) = E(t,z)\sqrt{v\mathrm{g}_g\Gamma_g/\gamma_q}$, $n_{g,q}(\tau,\zeta) = v\mathrm{g}_{g,q}\Gamma_{g,q}\left[N_r(t,z) - N_r^{tr}\right]/\gamma_q$, $j_g = v\mathrm{g}_g\Gamma_g\left(J_g - \gamma_g N_g^{tr}\right)/\gamma_q^2$, $j_q = v\mathrm{g}_g\Gamma_g N_q^{tr}/\gamma_q$, and $\Gamma = \gamma_g/\gamma_q$. The parameter $s = (\mathrm{g}_q\Gamma_q)/(\mathrm{g}_g\Gamma_g)$ is the ratio of the saturation intensities in the gain and absorber sections.

In the new coordinates (τ,ζ) Eq. (3) for the two passive sections takes the form:

$$\frac{\partial A(\tau,\zeta)}{\partial \zeta} = 0. \tag{10}$$

Solving Eqs. (6)-(10) and Eq. (4) the transformation of the electric field envelope by each of the five laser sections can be described. According to Eq. (10), the relation between input and output field in the two passive sections is given by

$$A(\tau,\zeta_2) = A(\tau,\zeta_1), \quad A(\tau,\zeta_5) = A(\tau,\zeta_4). \tag{11}$$

The transformations of the electric field envelope by the absorber and gain sections are obtained by integration of Eqs. (6) and (8)

$$A(\tau,\zeta_3) = e^{-\frac{1-i\alpha_q}{2}Q(\tau)} A(\tau,\zeta_2), \; A(\tau,\zeta_4) = e^{\frac{1-i\alpha_g}{2}G(\tau)} A(\tau,\zeta_3). \tag{12}$$

Here the dimensionless quantities $Q(\tau)$ and $G(\tau)$ describe saturable loss and gain introduced by the absorber and gain section respectively [23, 24]. They are given by

$$Q(\tau) = \int_{\zeta_2}^{\zeta_3} n_q(\tau,\zeta)\, d\zeta, \; G(\tau) = \int_{\zeta_3}^{\zeta_4} n_g(\tau,\zeta)\, d\zeta.$$

Integrating Eq. (9) over ζ from $\zeta_2 = z_2\gamma_q/v$ to $\zeta_3 = z_3\gamma_q/v$ and using the relation $\int_{\zeta_2}^{\zeta_3} n_q(\zeta,\tau)\,|A(\tau,\zeta)|^2\, d\zeta = -|A(\zeta_3,\tau)|^2 + |A(\zeta_2,\tau)|^2$ which follows from Eq. (6), we derive an equation governing evolution of the saturable loss:

$$\partial_\tau Q(\tau) = -q_0 - Q(\tau) + s\,|A(\tau,\zeta_3)|^2 - s\,|A(\tau,\zeta_2)|^2. \tag{13}$$

Here the unsaturated absorption parameter is defined by $q_0 = \int_{\zeta_2}^{\zeta_3} j_q d\zeta$. An equation for $G(\tau)$ is obtained in a similar way. It is given by

$$\partial_\tau G(\tau) = g_0 - \Gamma G(\tau) - |A(\tau,\zeta_4)|^2 + |A(\tau,\zeta_3)|^2, \tag{14}$$

with unsaturated gain (pump) parameter $g_0 = \int_{\zeta_3}^{\zeta_4} j_g d\zeta$.

Being rewritten in the time domain Eq. (4) for the spectral filtering section takes the following form

$$A(\tau,\zeta_1+T) = \int_{-\infty}^{\tau} f(\tau-\theta) A(s,\zeta_5)\, d\theta, \tag{15}$$

where $T = \gamma_q L/v$ is the normalized cavity round trip time (cavity length) and $f(\tau)$ is assumed to decay at $\tau \to \infty$ sufficiently fast, so that the integral in right hand side of Eq. (15) converges.

Substituting Eqs. (11) and (12) into Eq. (15) and using the periodic boundary condition (5) which can be rewritten in the form

$$A(\tau,\zeta+T) = A(\tau+T,\zeta),$$

we obtain the transformation of the electric field envelope $A(\tau) \equiv A(\tau,\zeta_1)$ after a complete round trip in the cavity

$$A(\tau+T) = \sqrt{\kappa}\int_{-\infty}^{\tau} f(\tau-\theta)\exp\left[\frac{1-i\alpha_g}{2}G(\theta) - \frac{1-i\alpha_q}{2}Q(\theta)\right] A(\theta)\, d\theta. \tag{16}$$

Here the attenuation factor $\kappa < 1$ describes non-resonant linear intensity losses per cavity round trip.

The equations governing the evolution of the saturable gain and loss are obtained from Eqs. (14) and (13) by using Eqs. (11) and (12) to express $A(\tau,\zeta_2)$, $A(\tau,\zeta_3)$, and $A(\tau,\zeta_4)$ in terms of $A(\tau) = A(\tau,\zeta_1)$. They read

$$\partial_\tau G(\tau) = g_0 - \Gamma G(\tau) - e^{-Q(\tau)}\left(e^{G(\tau)} - 1\right)|A(\tau)|^2, \tag{17}$$

$$\partial_\tau Q(\tau) = -q_0 - Q(\tau) - s\left(1 - e^{-Q(\tau)}\right)|A(\tau)|^2. \tag{18}$$

Eqs. (16)-(18) describe passive ML in a ring laser with arbitrary lineshape of the spectral filtering element defined by the linear response function $f(\tau)$. In the case when spectral filtering element is absent, this function can be replaced by the Dirac delta function, $f(\tau) = \delta(\tau)$. Then Eq. (16) is transformed into

$$A(\tau+T) = \sqrt{\kappa} e^{\frac{1-i\alpha_g}{2}G(\tau-T) - \frac{1-i\alpha_q}{2}Q(\tau-T)} A(\tau). \tag{19}$$

which is similar to the map introduced by Ikeda [25, 26]. Eqs. (19), (17), and (18) describe passive ML in a laser without spectral filtering element, i.e. in a situation considered by New [3]. A ML solution of these equations can be expressed in terms of the Dirac delta function $|A(\tau)|^2 = \Delta P \sum_{n=-\infty}^{\infty} \delta(\tau - nT)$, where ΔP is the dimensionless energy of a ML pulse. This solution is characterized by infinitely

large number of locked modes and infinitely short pulse with repetition period equal precisely to cold cavity round trip time T.

Now let us consider the case when the response function in Eq. (16) is defined by

$$f(\tau) = \begin{cases} \frac{\gamma}{1-e^{-\gamma\Delta}} e^{(-\gamma+i\Omega)\tau}, & 0 \le \tau \le \Delta \\ 0, & \tau > \Delta \end{cases}, \tag{20}$$

where the parameter Ω describes the detuning of the central frequency of the spectral filtering element. In this case Eqs. (16)-(18) can be replaced by a set of delay differential equations (DDEs) with two delays:

$$\begin{aligned} \partial_\tau A(\tau) + (\gamma - i\Omega) A(\tau) &= \frac{\gamma\sqrt{\kappa}}{1-e^{-\gamma\Delta}} \left[e^{\frac{1-i\alpha_g}{2} G(\tau-T) - \frac{1-i\alpha_q}{2} Q(\tau-T)} A(\tau-T) \right. \\ &\left. - e^{(-\gamma+i\Omega)\Delta} e^{\frac{1-i\alpha_g}{2} G(\tau-T_1) - \frac{1-i\alpha_q}{2} Q(\tau-T_1)} A(\tau-T_1) \right] \end{aligned} \tag{21}$$

Here $T_1 = T + \Delta$. The solution of Eq. (21) can be written in the form

$$A(\tau+T) = e^{(-\gamma+i\Omega)\tau} \left[C + \frac{\gamma\sqrt{\kappa}}{1-e^{-\gamma\Delta}} \int_{\tau-\Delta}^{\tau} e^{(\gamma-i\Omega)\theta + \frac{1-i\alpha_g}{2} G(\theta) - \frac{1-i\alpha_q}{2} Q(\theta)} A(\theta)\, d\theta \right]. \tag{22}$$

One can see from Eq. (22) that in order Eq. (21) be equivalent to Eq. (16) the equation $C = 0$ must be satisfied. This implies the following initial condition for the electric field envelope

$$A(0) = \frac{\gamma\sqrt{\kappa}}{1-e^{-\gamma\Delta}} \int_{-T_1}^{-T} e^{(\gamma-i\Omega)\tau + \frac{1-i\alpha_g}{2} G(\tau) - \frac{1-i\alpha_q}{2} Q(\tau)} A(\tau)\, d\tau. \tag{23}$$

Eq. (23) defines the initial condition for which Eqs. (21) are equivalent to Eq. (16). However, since, for $\gamma > 0$ the term proportional to C in Eq. (22) decays exponentially as $\tau \to \infty$, its precise form can be safely dismissed in the calculations.

In order to clarify the physical meaning of (20) let us consider two limiting situations. In the limit $\gamma \to 0$ the function $f(\tau)$ becomes a stepwise one with the Fourier transform $\widehat{f}(\omega) \propto e^{-i\omega\Delta/2} \sin(\omega\Delta/2) / (\omega\Delta/2)$. Such a function describes a reflection from weak Bragg grating. Note, however, that for $\gamma = 0$ the term proportional to C in Eq. (22) does not decay with time. Therefore, in this case, unlike the case when $\gamma > 0$, one has to choose the precise form of the initial condition defined by Eq. (23) in order to get a correct result.

The second situation, $\Delta \to \infty$, corresponds to Lorentzian lineshape of the bandwidth limiting element, $f(\tau) = \gamma e^{(-\gamma+i\Omega)\tau}$. In this case Eqs. (16)-(18) can be replaced by a set of DDEs with a single delay parameter equal to the cavity round trip time T. After the coordinate change $A \to A e^{i\Omega\tau}$ this set takes the form

$$\gamma^{-1} \partial_\tau A(\tau) + A(\tau) = \sqrt{\kappa} e^{\frac{1-i\alpha_g}{2} G(\tau-T) - \frac{1-i\alpha_q}{2} Q(\tau-T) - i\varphi} A(\tau-T), \tag{24}$$

$$\partial_\tau G(\tau) = g_0 - \Gamma G(\tau) - e^{-Q(\tau)} \left(e^{G(\tau)} - 1 \right) |A(\tau)|^2, \tag{25}$$

$$\partial_\tau Q(\tau) = -q_0 - Q(\tau) - s \left(1 - e^{-Q(\tau)} \right) |A(\tau)|^2, \tag{26}$$

with $\varphi = \Omega T$. In the following we restrict our consideration to the analysis of Eqs. (24)-(26).

2 Limit of infinitely broad bandwidth

The number of cavity modes that take part in ML process can be roughly estimated through the ratio of the bandwidth of the spectral filtering element, γ, and the cavity intermode frequency spacing, T^{-1}. In this section we perform analytical study of Eqs. (24)-(26) in the case when T is fixed and $\gamma \to \infty$. In this limit the duration of a ML pulse vanishes, $\tau_p \propto \gamma^{-1}$, its amplitude diverges, $A_0 \propto \gamma^{1/2}$, while the pulse energy, $\Delta P \propto A_0^2 \tau_p$, remains finite. Physically this means that the number of locked laser modes grows, but at the same time the energy associated with each mode taken separately decreases.

If γ is sufficiently large and the relaxation times of the intracavity media are large as compared with the pulse duration (slow absorber), then following the approach of New [3] and Haus [2], we split the evolution of a ML solution into two stages. At the slow stage the amplifying and absorbing media recover slowly between two subsequent pulses. During this stage the electric field intensity is close to zero, $|A(\tau)|^2 \approx 0$ (see Fig. 2). Therefore, the terms proportional to $|A(\tau)|^2$ in Eqs. (25) and (26) can be neglected at the slow stage. At the short fast stage the electric field intensity is large and therefore, the terms proportional to $|A(\tau)|^2$ dominate in the right hand sides of Eqs. (25) and (26). The remaining relaxation terms can be neglected at the fast stage.

When γ increases the duration of the slow stage tends to the cavity round trip time T, while the duration of the fast phase vanishes. New solved the laser equations for the two stages separately and calculated the energy of the pulse ΔP by gluing the two solutions [3]. He also proposed a stability criterion for ML pulses. According to this criterion they are stable if the net gain $G(\tau) - Q(\tau) + \ln \kappa$ is negative during the entire slow stage. Physically this means that small perturbations of the low intensity background between ML pulses decay with time (absolute stability). It can be shown that the New's background stability criterion is fulfilled if the net gain is negative at the beginning and at the end of the slow stage. Therefore, this criterion can be rewritten as a set of two inequalities

$$G_1 - Q_1 + \ln \kappa < 0, \tag{27}$$

$$G_2 - Q_2 + \ln \kappa < 0. \tag{28}$$

Here G_2 and Q_2 (G_1 and Q_1) are the saturable gain $G(\tau)$ and loss $Q(\tau)$ evaluated at the beginning (end) of the slow stage (see Fig. 2). Since the end of the slow stage corresponds to the beginning of the fast one and vice versa, the inequalities (27) and (28) give the background stability conditions at the leading and trailing edge of a pulse, respectively.

Linear ordinary differential equations that describe the evolution of $G(\tau)$ and $Q(\tau)$ at the slow stage are easily integrated. However, Eq. (24) describing evolution of the electric field amplitude at the fast stage cannot be solved analytically without further

approximations. The approach of New assumes the absence of spectral filtering in the cavity. In this case $f(\tau) = \delta(\tau)$ in Eq. (16) and, therefore, this equation is transformed into Eq. (19). Such approximation is equivalent to the neglect of the derivative term $\gamma^{-1}\partial_\tau A(\tau)$ in Eq. (24). Note, however, that for a ML solution this term remains finite for $\gamma^{-1} \to 0$, and, therefore, cannot be neglected even in the limit of infinitely broad bandwidth. To illustrate this statement let us consider a ML solution having time periodic intensity, $|A(\tau + T_p)|^2 = |A(\tau)|^2$, with the period T_p close to the cavity round trip time T. Substituting this solution into Eq. (24), taking modulus square from both sides, and integrating over the period T_p we obtain

$$\gamma^{-2} \int_0^{T_p} |\partial_\tau A(\tau)|^2 \, d\tau + \Delta P = \kappa \int_0^{T_p} e^{G(\tau) - Q(\tau)} |A(\tau)|^2 \, d\tau, \tag{29}$$

where $\Delta P = \int_0^{T_p} |A(\tau)|^2 \, d\tau$ is the total dimensionless energy of the ML pulse. Eq. (29) is similar to Eq. (46) of Ref. [2] which was derived under assumptions of parabolic dispersion, small gain and loss per round trip, and weak saturation. The integral in the left hand side of Eq. (29) describes energy losses introduced by spectral filtering element. As it was pointed out by Haus [2], in the limit of infinitely broad bandwidth one gets $|\partial_\tau A(\tau)|^2 \propto \gamma^2 |A(\tau)|^2$ and, hence, these losses, neglected by New, remain finite. Physically this means that the spectral width of a ML pulse increases with the bandwidth of the spectral filtering element, so that the losses introduced by this element remain finite.

Since the electric field intensity is very small during the slow stage, the integration in Eq. (29) can be restricted to the fast stage only. Then using the solutions for G and Q obtained in section 2.2, the integral in the right hand side of Eq. (29) can be expressed analytically in terms of the total pulse energy ΔP. The integral in the left hand side, however, can be calculated analytically only in the limit of weak saturation that underlies Haus' theory (see section 2.4).

Below we demonstrate that under certain approximations the background stability domains of ML solutions calculated analytically using Eqs. (24)-(26) coincide with those derived by New [3] and Haus [2]. Moreover, our DDE model allows to generalize their analytical results to the case when gain and loss per cavity round trip are not small, i.e. to a situation typical of semiconductor lasers. This is done in sections 2.3 and 2.4.

2.1 Slow stage

Let us consider a solution of Eqs. (24)-(26) with periodic laser intensity corresponding to a ML regime (see Fig. 2). Between two subsequent pulses, when the amplitude of the electric field is close to zero, $|A(\tau)|^2 \approx 0$, the equations for the saturable gain and loss become linear

$$\partial_\tau G(\tau) = g_0 - \Gamma G(\tau), \; \partial_\tau Q(\tau) = -q_0 - Q(\tau). \tag{30}$$

Solving Eqs. (30) we express the saturable gain and loss at the end of the slow stage, G_1 and Q_1, via their values at the beginning of this stage, G_2 and Q_2:

$$G_1 = G_2 e^{-\Gamma T} + \frac{g_0}{\Gamma}\left(1 - e^{-\Gamma T}\right), \tag{31}$$

$$Q_1 = Q_2 e^{-T} - q_0\left(1 - e^{-T}\right). \tag{32}$$

Here T is the duration of the slow phase equal to the cavity round trip time in the limit $\gamma \to \infty$.

Eqs. (31), (32) can be further simplified in two limiting cases:

(i) Absorber relaxes completely between two subsequent pulses, $T \ll 1$. Then instead of Eq. (32) we obtain

$$Q_1 = -q_0. \tag{33}$$

(ii) The relaxation time of the gain medium is much smaller than the cavity round trip time, $\Gamma T \ll 1$. In this case Eq. (31) is replaced by

$$G_1 = G_2 + g_0 T. \tag{34}$$

2.2 Fast stage

The duration of the fast stage coincides with the pulse width τ_p (see Fig. 2). Since under the slow absorber approximation τ_p is assumed to be small as compared with the relaxation times of amplifying and absorbing media and the electric field intensity is large during the fast stage, the relaxation terms in the right hand sides of Eqs. (25) and (26) can be neglected at this stage. Then, introducing dimensionless differential pulse energy $P(\tau) = \int_0^\tau |A(\theta)|^2 d\theta$, where $\tau = 0$ corresponds to the beginning of the fast stage, we rewrite Eqs. (25) and (26) in the form

$$\partial_P g(P) = -e^{-q(P)}(e^{g(P)} - 1),\ \partial_P q(P) = -s\left(1 - e^{-q(P)}\right), \tag{35}$$

with $g(P) = G(\tau)$ and $q(P) = Q(\tau)$. Using the solutions of Eqs. (35) we express the saturable gain and loss at the end of the fast stage (trailing edge of a pulse), $G_2 = g(\Delta P)$ and $Q_2 = q(\Delta P)$, via their values, $G_1 = g(0)$ and $Q_1 = q(0)$, at the beginning of this stage (leading edge of a pulse)

$$G_2 = g(\Delta P) = -\ln\left\{1 - \frac{1 - e^{-G_1}}{\left[e^{-Q_1}\left(e^{s\Delta P} - 1\right) + 1\right]^{1/s}}\right\}, \tag{36}$$

$$Q_2 = q(\Delta P) = \ln\left[1 + e^{-s\Delta P}\left(e^{Q_1} - 1\right)\right]. \tag{37}$$

Here $\Delta P = P(\tau_p) = \int_0^{\tau_p} |A(\tau)|^2 d\tau$ is the total dimensionless energy of a ML pulse. Substituting the solutions of Eqs. (35) into the right hand side of Eq. (29) and performing integration we obtain

$$\kappa \int_0^{T_p} e^{G(\tau)-Q(\tau)} |A(\tau)|^2 d\tau = \kappa \int_0^{\Delta P} e^{g(P)-q(P)} dP = \kappa \ln \frac{e^{G_1}-1}{e^{G_2}-1}.$$

Therefore, instead of Eq. (29) we get

$$\gamma^{-2} \int_0^{\tau_p} |\partial_\tau A(\tau)|^2 d\tau + \Delta P = \kappa \ln \frac{e^{G_1}-1}{e^{G_2}-1}. \tag{38}$$

In order to solve Eqs. (31), (32), and (36)-(38) for the pulse parameters, $G_{1,2}$, $Q_{1,2}$ and ΔP, one has to express the integral in the left hand side of Eq. (38) in terms of these five unknowns. Two particular situations in which this can be done analytically are described in the following two sections, 2.3 and 2.4.

2.3 A generalization of New's model

As it was already mentioned, the neglect of spectral filtering in New's approach [3] is equivalent to the neglect of the integral term in the left hand side of Eq. (38). Then this equation becomes

$$\Delta P = \kappa \ln \frac{e^{G_1}-1}{e^{G_2}-1}. \tag{39}$$

Together with Eq. (39), Eqs. (31), (32), (36), and (37) constitute a closed set of equations that can be solved for $G_{1,2}$, $Q_{1,2}$ and ΔP. This gives the dependence of the pulse energy ΔP on the laser parameters. Substituting the solution into inequalities (27) and (28) one can calculate background stability boundaries of a ML pulse. A result of such a calculation is presented in Fig. 3 for the ML solutions with the period T and $T/2$. The first of them corresponds to a fundamental ML regime with a single pulse circulating in the cavity, while the second one corresponds to a regime with twice greater repetition rate and two pulses in the cavity. One can see that the two stability domains overlap in a certain parameter range. This means that there may be a hysteresis between regimes having different repetition rates. According to Fig. 3, the two background stability boundaries, namely those for the leading and trailing edge of a pulse, meet each other at a codimension two point. This point lying on the lasing threshold line Th can be calculated explicitly

$$q_0 = -\ln \frac{\kappa(s-1)}{s\kappa-1}, \;\; g_0 = \Gamma \ln \frac{s-1}{s\kappa-1}. \tag{40}$$

It is well known [17] that ML pulses with stable background can exist only if the absorbing medium is saturated faster than the gain one [2], i.e. when

$$s > 1. \tag{41}$$

It follows from Eqs. (40) that in a situation when gain and loss per cavity round trip are not small, the existence of such pulses is possible only if an additional condition

$$s\kappa > 1, \tag{42}$$

is satisfied. In the small gain and loss limit, $\kappa \to 1$, this new condition coincides with (41). However, for the parameter values typical of semiconductor lasers with their high losses, $\kappa \ll 1$, the inequality (42) implies much stronger limitation on the minimal value of the ratio of saturation intensities than the previously known condition (41).

Eqs. (31), (32), (36), (37) and (39) can be considered as a generalized New's model because unlike the equations for the pulse parameters derived in Ref. [3] they do not assume that gain and loss per round trip are small. In order to recover from these equations those obtained by New we expand Eqs. (36), (37) up to the first order terms in G_1 and Q_1:

$$G_2 = G_1 e^{-\Delta P},\ Q_2 = Q_1 e^{-s\Delta P}. \tag{43}$$

Then, substituting Eq. (36) into Eq. (39) and expanding it up to the first order terms in G_1, Q_1, and $\ln\kappa$ we obtain the equation for the pulse energy

$$G_1\left(1 - e^{\Delta P}\right) - Q_1\frac{\left(1 - e^{s\Delta P}\right)}{s} - \Delta P \ln\kappa = 0, \tag{44}$$

which is equivalent to Eqs. (11) and (12) of Ref. [3].

Background stability boundaries of ML pulses calculated using four different sets of equations are presented in Fig. 4. In this figure solid lines labeled L_N and T_N indicate the leading and trailing edge instability boundaries obtained with the pulse parameters calculated using Eqs. (31), (33), (43), and (44). These equations are equivalent to the original equations derived by New [3]. Solid lines labeled L_{NG} and T_{NG} have been calculated using the generalization of New's model described in this section. The dots in Fig. 4 represent points at the background stability boundaries which have been calculated by means of direct numerical integration of Eqs. (24)-(26) with $\gamma = 333$. Noteworthy is that with the decrease of γ the width of the background stability domain increases. One can see from Fig. 4 that the generalized New's model appears to be in a quite good agreement with the results of numerical integration of the DDE model. On the other hand, discrepancy between the numerical data and the results obtained using the original New's equations [3] is very pronounced. This is because Fig. 4 corresponds to parameter values typical of semiconductor lasers in which gain and loss per round trip are large. The dotted lines in Fig. 4 indicate background stability boundaries obtained using the original Haus' equations [2] and a generalization of those equations derived in the next section.

Note that it follows from our consideration that in the framework of New's approach, in which the derivative term is neglected in Eq. (24), the background stability boundaries do not depend on the linewidth enhancement factors. This is not true

any more as soon as spectral filtering is taken into account. However, for simplicity we restrict our consideration below to the case when $\alpha_{g,q} = 0$ and $\varphi = 0$ in Eq. (24). In particular, this means that one of the cavity eigenfrequencies coincides with the central frequency of the spectral filtering element.

2.4 A generalization of Haus' model

In this section we study a situation when gain and absorbing media are weakly saturated by ML pulses. In this case using Haus' approach one can obtain an explicit expression for ML pulse shape by solving analytically the ML equations for the fast stage. Let us consider a periodic ML solution, $A(\tau + T) = A(\tau - \delta T)$, where $\delta T = T_p - T$ is the small difference between the pulse repetition period T_p and the cavity round trip time. Substituting this solution into Eq. (24) we obtain

$$\gamma^{-1}\partial_\tau A(\tau - \delta T) + A(\tau - \delta T) = \sqrt{\kappa} e^{\frac{g(P)-q(P)}{2}} A(\tau). \tag{45}$$

In Eq. (45) $g(P)$ and $q(P)$ are the solutions of Eqs. (35). In the limit $\gamma \to \infty$ corresponding to infinite bandwidth of the spectral filtering element the duration of the pulse vanishes and the period of ML solution tends to the cavity round trip time, i.e., $\tau_p, \delta T \propto \gamma^{-1}$. Introducing in this limit a rescaled time variable $\xi = \gamma\tau$ we rewrite Eq. (45) in the form

$$\partial_\xi a(\xi - c) + a(\xi - c) = \sqrt{\kappa} F(P(\xi)) a(\xi), \tag{46}$$

where $a(\xi) = \gamma^{-1/2} A(\tau)$, $P(\xi) = \int_{-\infty}^{\xi} |a(s)|^2 ds$, and $c = \lim_{\gamma\to\infty}(\gamma\delta T)$. The function $F(P)$ is obtained by solving Eqs. (35) and substituting their solutions into Eq. (45):

$$F(P) = \left\{ \left[1 + e^{-sP(\xi)}\left(e^{Q_1} - 1\right)\right] \left[1 - \frac{1 - e^{-G_1}}{\left(e^{sP(\xi)-Q_1} - e^{-Q_1} + 1\right)^{1/s}}\right] \right\}^{-1/2}. \tag{47}$$

Eqs. (46) and (47) describe a ML pulse shape in the limit of infinitely broad Lorentzian bandwidth. For a laser operating close enough to the threshold the normalized pulse energy is small $P(\zeta), \Delta P \ll 1/s$, which means that both the absorber and amplifier are weakly saturated. Under this approximation, which underlies Haus' theory [2], Eqs. (36) and (37) together with the function $F(P)$ in Eq. (46) can be expanded in power series up to the second order terms in the pulse energy. This yields

$$G_2 = G_1 + g'(0)\Delta P + \frac{g''(0)}{2}\Delta P^2, \tag{48}$$

$$Q_2 = Q_1 + q'(0)\Delta P + \frac{q''(0)}{2}\Delta P^2, \tag{49}$$

$$c\partial_{\zeta\zeta} a(\xi) - (1 - c)\partial_\xi a(\xi) + \left[F(0) + F'(0)P(\xi) + \frac{F''(0)}{2}P(\xi)^2\right] a(\xi) = 0. \tag{50}$$

Here the functions g, q, and F are defined by Eqs. (36), (37), and (47), respectively. In Eq. (50) we have used an approximation $a(\zeta - c) \approx a(\zeta) - ca_\zeta(\zeta)$ that is equivalent to the assumption that the gain dispersion is parabolic. Such approximation is valid for a laser operating near the threshold. A solution of Eq. (50) can be written in the form [2]:

$$a(\xi) = \sqrt{\frac{\Delta P}{2\xi_p}} \operatorname{sech}\left(\frac{\xi}{\xi_p}\right), \tag{51}$$

where $\xi_p = \gamma\tau_p$ is the normalized pulsewidth. At this solution the integral term in the left hand side of Eq. (38) becomes $\Delta P/3\tau_p^2$. Substituting Eq. (51) into Eq. (50) and equating coefficients in front of different powers of hyperbolic tangent we obtain three equations for three unknown parameters: the normalized pulse energy ΔP, the pulsewidth ξ_p, and the coefficient c which describes the second order dispersion. Elimination of the two latter parameters leads to a second order equation for the pulse energy

$$r_0 + r_1\Delta P + r_2\Delta P^2 = 0, \tag{52}$$

with

$$r_0 = 2\left(\sqrt{\kappa}e^{\frac{G_2-Q_2}{2}} - 1\right), \tag{53}$$

$$r_1 = \frac{1}{2}\sqrt{\kappa}e^{\frac{G_2-Q_2}{2}}\left[e^{-Q_2}\left(1 - e^{G_2}\right) + s(1 - e^{-Q_2})\right], \tag{54}$$

$$\begin{aligned} r_2 = {} & \frac{3}{32}\sqrt{\kappa}e^{\frac{3(G_2-Q_2)}{2}}\left[3e^{G_2-Q_2} + s^2e^{Q_2-G_2}\right. \\ & \left. + \left(3s^2 - 4s + 1\right)e^{-G_2-Q_2} + 4(s-1)e^{-Q_2} - 4s(1-s)e^{-G_2} - 4s\right]. \end{aligned} \tag{55}$$

Since in the derivation of Eqs (52), (31), (32), (36), and (37) we have not used small gain and loss approximation they can be considered as a generalization of Haus' model [2]. Solving these equations for the pulse parameters $G_{1,2}$, $Q_{1,2}$, and ΔP and substituting their solutions into the inequalities (27) and (28) we get background stability boundaries for the sech-solution defined by Eq. (51). It follows from Eq. (53) that the equation $r_0 = 0$, corresponds to zero net gain at the trailing edge of a pulse. Hence, this equation defines the trailing edge instability boundary of ML pulse. Furthermore, according to Eq. (52), the two equations $r_0 = 0$ and $r_1 = 0$ define a codimension-two point where the trailing edge instability boundary hits the lasing threshold. Solving these equations for G_2 and Q_2 and taking into account that at $\Delta P = 0$ one has $G_1 = G_2 = g_0/\Gamma$ and $Q_1 = G_2 = -q_0$ we recover the codimension two point (40). Hence, the tips of the background stability tongues calculated using the generalized New's and the generalized Haus' approaches are located at the same point in the parameter space.

In the limit of small gain and loss per cavity round trip the generalized model derived in this section is reduced to the original Haus' equations. To demonstrate this we expand Eqs. (48) and (49) up to the first order terms in G_1 and Q_1:

$$G_2 = G_1 \left(1 - \Delta P + \frac{1}{2}\Delta P^2\right), \tag{56}$$

$$Q_2 = Q_1 \left(1 - s\Delta P + \frac{s^2}{2}\Delta P^2\right), \tag{57}$$

Then, expanding Eqs. (53)-(55) into power series up to the first order terms in G_2, Q_2, and $\ln\kappa$ we obtain an equation for the normalized pulse energy equivalent to Eq. (36) of Ref. [2]:

$$G_2 - Q_2 + \ln\kappa + \frac{1}{2}\left(G_2 - sQ_2\right)\Delta P - \frac{3}{16}\left(G_2 - s^2 Q_2\right)\Delta P^2 = 0. \tag{58}$$

In Fig. 4 leading and trailing edge instability boundaries calculated using the original Haus' equations [2] are shown by the dotted lines L_H and T_H, respectively. The same boundaries obtained using the generalization of the Haus' model described in this section are indicated by the dotted lines L_{HG} and T_{HG}. One can see that similarly to the original New's model the original Haus' model is not applicable to describe ML in a parameter domain typical of semiconductor lasers. According to the figure, the generalized Haus' equations work well only when the pulse energy is small enough. The discrepancy between the background instability boundaries calculated using these equations and the results of direct numerical integration of Eqs. (24)-(26) increases with the increase of the pulse energy. On the other hand, the results obtained using the generalized New's approach remain in quite good agreement with those of direct numerical simulations even under strong saturation condition.

3 Numerical results

In this section we present some results of numerical analysis of Eqs. (24)-(26) with $T = 2.5$, $\kappa = 0.1$, $\Gamma = 1.33 \cdot 10^{-2}$, $\gamma = 33.3$, $\alpha_{g,q} = 0$, and $\varphi = 0$. A situation when the linewidth enhancement factors are non-zero will be a subject of a separate investigation. We have used the RADAR5 code [27] to solve these equations numerically and the DDEBIFTOOL package [28] to trace their bifurcations in the parameter space. The simplest stationary solution of Eqs. (24)-(26) is the one corresponding to zero electric field intensity:

$$A = 0,\ G = g_0/\Gamma,\ Q = -q_0. \tag{59}$$

This solution corresponds to laser off. The stability of the steady state (59) is determined by the roots of the characteristic equation

$$\lambda + \gamma\left(1 - \sqrt{\kappa} e^{\frac{g_0}{\Gamma} - q_0 - \lambda T}\right) = 0. \tag{60}$$

It follows from Eq. (60) that the steady state (59) is stable when

$$g_0 < \Gamma \left(\ln \kappa - q_0 \right). \tag{61}$$

The inequality (60) defines the lasing threshold where so-called constant wave (CW) solution characterized by time-independent nonzero laser intensity bifurcates from the steady state (59) with the increase of the pump parameter g_0. The intensity of the CW solution $I = |A|^2$ obeys the implicit relation:

$$\ln \left[\frac{I \, (s\,\Gamma - 1)}{\sqrt{\kappa}\,\Gamma \, \left(I\, s + \frac{\ln \kappa}{2} \, - g_0 \right) - (I + q_0 \, \sqrt{\kappa})} \right] \tag{62}$$

$$= \frac{s \, \left(g_0 + I - \frac{I}{\sqrt{\kappa}} \right) + \frac{\ln \kappa}{2} \, + \, q_0}{s\,\Gamma - 1}. \tag{63}$$

The CW solution is stable when the pump parameter g_0 is large enough as compared to the absolute value $|q_0|$ of the unsaturated loss parameter. This corresponds to a situation when the amount of saturable absorption is not sufficient to destabilize CW operation. With the increase of saturable losses $|q_0|$ the CW solution can exhibit Hopf bifurcations leading to solutions with time periodic intensity. In Fig. 5 Hopf bifurcation curve H_1 gives rise to a periodic solution that, when stable, corresponds to a fundamental ML regime with the pulse repetition period close to the cavity round trip time T. The Hopf bifurcation curves H_n with $n = 2, 3, 4$ signal the onset of multiple pulse ML regimes with the repetition periods $T_n \approx T/n$. The curve H_Q indicates a Hopf bifurcation with the period approximately one order of magnitude greater than T for the parameter values of Fig. 5. This frequency is associated with Q-switching instability. The dots in Fig. 5 have been calculated by direct numerical integration of Eqs. (24)-(26). They represent points on the Q-switching instability boundary of the fundamental ML regime. One can see that this boundary turns out to be quite close to the Hopf bifurcation curve H_Q of the CW solution.

The results of direct numerical integration of the DDE model are presented in Figs. 6-8. Bifurcation diagram in Fig. 6 shows extrema of time dependence of laser intensity calculated for different values of the pump parameter g_0. To calculate this diagram we have used the following procedure. First, Eqs. (24)-(26) have been integrated from $\tau = 0$ to $\tau \approx 2 \cdot 10^3$ in order to skip transient behavior. After that, during the time interval $\Delta\tau \approx 200$, maxima and minima of the intensity time trace have been plotted for each given value of g_0. It follows from Fig. 6 that when the pump parameter g_0 is small enough, $0.09 < g_0 < 1.13$, the laser exhibits a regime with pulse power modulated in time by the Q-switching frequency. Intensity timetrace illustrating this regime is shown in Fig. 8a. With the increase of g_0 modulation disappears at a secondary Hopf bifurcation point $g_0 \simeq 1.13$ and a transition to a fundamental periodic ML regime occurs. This regime is shown in Fig. 7a. With further increase of the pump parameter transitions to regimes with approximately twice and thrice higher pulse repetition frequency take place at $g_0 \simeq 2.99$ and $g_0 \simeq 4.01$, respectively. These regimes shown in Fig. 7b and Fig. 7c

are characterized by the pulse peak intensities smaller than that of the fundamental ML regime. The break up of ML behavior occurs at $g \simeq 4.15$ with the appearance of nonperiodic modulation of the pulse power (see the intensity timetrace shown in Fig. 8b). Finally, at large gains, $g_0 > 5.2$, the laser undergoes a transition to CW operation with the electric field intensity independent of time. The bifurcation diagram in Fig. 6 appears to be in a qualitative agreement with the experimental results of Refs. [32, 33] where a gradual transition from a ML regime to a selfpulsing one was observed with the increase of the injection current in the gain section. A regime with the repetition period equal approximately to one half of the cavity round trip time was also observed experimentally in a passively mode-locked ring semiconductor laser [34].

Fig. 9 shows time traces of the electric field intensity and the round trip net gain parameter $G(\tau) - Q(\tau) + \ln \kappa$ for two different fundamental ML regimes. In Fig. 9a corresponding to $g_0 = 0.6$ the net gain is negative between pulses and becomes positive only during a short time interval when the pulse amplitude is large. Therefore, the solution shown in this figure has "stable" background according to New's criterion. Perturbations of the low intensity background between these pulses do not grow with time. On the contrary, Fig. 9b corresponding to $g_0 = 1.33$ represents a stable periodic solution of Eqs. (24)-(26) having "unstable" background. The existence of stable ML pulses with "unstable" background at the trailing edge was reported earlier in Refs. [13, 20]. Fig. 9b corresponds to the case when the net gain is positive at the leading edge of a ML pulse. This behavior is similar to the phenomenon of delayed loss of stability which is typical of singularly perturbed dynamical systems [29]. In a model of a laser with a saturable absorber the effect of delayed stability loss was studied in Ref. [30]. For periodic solutions corresponding to Q-switching regimes in this model the phase trajectory spends most time near the slow manifold $A = 0$, which is split into stable and unstable parts. Stability is accumulated when the phase trajectory goes along the stable part of the slow manifold. After a transition to the unstable part, the phase trajectory continues to stay near the slow manifold for a certain time interval until a critical amount of instability is accumulated for the pulse development. Similar behavior is observed in Fig. 9b where the net gain window is opened well before the arrival of a pulse in the course of the carrier density relaxation process. Since for the parameter values typical of semiconductor lases the gain recovers much slower than the absorption, it continues to recover when the absorption is already almost completely recovered to its unsaturated value. As a result, a net gain window appears. Such behavior is quite different from the classical ML mechanism described in [3] and illustrated by Fig. 9a.

Obviously, stable ML solutions with "unstable" background can exist only when the group velocity of the pulses v_p is different from the group velocity v_0 of small perturbations of the low intensity background. Let us consider a ML regime with the period $T_p = T + \delta T$, close to the cold cavity round trip time T, i.e. $\delta T \ll T$.

Then the pulse group velocity can be estimated as

$$v_p = v\frac{T}{T_p} = v\left(1 - \frac{\delta T}{T_p}\right) \approx v\left(1 - \frac{\delta T}{T}\right).$$

Here v is the cold cavity group velocity, which enters Eqs. (1) and (2). For large γ the group velocity v_0 of small perturbations of the low intensity background can be estimated using the approximation $\partial_\tau A(\tau) + \gamma A(\tau) \approx \gamma A(\tau + \gamma^{-1})$ in the left hand side of Eq. (24). Then this equation becomes equivalent to Eq. (19) with the round trip time T replaced with $T + \gamma^{-1}$. Therefore, the round trip time for small perturbations is approximately equal to $T + \gamma^{-1}$, and, hence, the corresponding group velocity is

$$v_0 \approx v\frac{T}{T + \gamma^{-1}} \approx v\left(1 - \frac{1}{\gamma T}\right).$$

Note that the difference between v_0 and the cold cavity group velocity v arises due to the presence of spectral filtering element.

Dependence of normalized pulse group velocity v_p/v on the pump parameter g_0 for different values of the unsaturated loss parameter q_0 is shown in Fig. 10. Horizontal lines in this figure show the normalized group velocity $v_0/v \approx T/(T + \gamma^{-1})$ of small perturbations of the low intensity background (dotted line) and the normalized cold cavity group velocity (solid line). According to Fig. 10, the group velocity of the ML pulses with "unstable" leading edge shown in Fig 9b is greater than v_0. These pulses remain stable because small perturbations amplified at the leading edge are absorbed by a pulse in the course of propagation. The acceleration of a pulse by nonlinear intracavity media can be understood by observing that in Fig. 9b the net gain window is shifted to the leading edge of a pulse. Hence, the leading edge is amplified, while the trailing edge is attenuated.

The ML pulses shown in Fig. 9b have a group velocity smaller than that of the cold cavity, i.e. $\delta T > 0$. However, stable pulses with group velocities v_p greater than v are also possible when the pump parameter g_0 is large enough (see curve 1 in Fig. 10). Such pulses should always have "unstable" background at the leading edge. Indeed, if the period of the ML solution coincides with the round trip time, $T_p = T$, this solution obeys an ordinary differential equations that are given by Eqs. (24)-(26) with $\tau - T$ replaced with τ. Pulsed solutions of such ordinary differential equations without delay cannot have stable background.

Dependence of the ML pulsewidth as a function of the pump parameter is presented in Fig. 11. One can see that the width of the pulses having stable background decreases with the increase of the pump parameter. However, the appearance of the unstable background leads to an increase of the pulse width (see curves 1 and 2 in Fig. 11).

4 Conclusion

We have developed and studied a new model for passive ML – a set of three differential equations with time delay (24)-(26). This model can be considered as a generalization of Haus' master equation. Being more general than the models proposed earlier by New and Haus our model includes both of them as particular limits. An important feature of the delay differential model is that unlike Haus' master equation it does not assume small gain and loss per cavity round trip, low saturation, and infinitely broad spectral bandwidth. These approximations (especially the small gain and loss approximation) are hardly satisfied for semiconductor lasers. The only assumptions we retain concern Lorentzian lineshape of spectral filtering and ring cavity geometry. The latter approximation seems to be quite reasonable at least for qualitative consideration of ML unless colliding pulse ML devices are considered.

Our model allows of analytical description of the pulse background stability domain in the limit of infinite bandwidth of the spectral filtering element which is equivalent to the slow absorber approximation used by New and Haus. Using the approaches developed by these authors we have generalized their analytical results to the case when gain and loss per round trip are not small. In particular, this refers to the pulse background instability boundaries shown in Fig. 4, and the condition (42) which gives a generalization of the well known ML condition $s > 1$. According to our results, in the parameter range typical of semiconductor lasers background instability boundaries of ML pulses can be quite well approximated using the generalization of New's approach described in section 2.3.

Eqs. (24)-(26) can be easily simulated using standard codes developed for the solution of delay differential equations. The numerical results obtained are in qualitative agreement with the experimental data. We have found that stable ML pulses with positive net gain at the leading edge can exist for certain laser parameter values. Such pulses do not satisfy New's background stability criterion. Also they are expected to be much more affected by noise than usual ML pulses with "stable" background.

The delay differential model described in this paper can be easily modified to study active and hybrid ML or take into account such additional physical effects arising in semiconductor lasers as, for example, fast nonlinearities associated with intraband relaxation processes.

We are grateful to U. Bandelow, B. Hüttl, R. Kaiser, G. Kozyreff, D. Rachinskii, M. Radziunas, K. Schneider, E. Viktorov, M. Wolfrum, and S. Yanchuk for useful discussions. We would also like to thank T. Erneux for providing a copy us his paper prior to its publication.

References

[1] P. Vasil'ev, Ultrafast Diode Lasers: Fundamentals and Applications, Artech House Publishers, 1995.

[2] H.Haus, "Theory of mode locking with a slow saturable absorber", IEEE J. of Quantum Electron., **11**, 736-746 (1975).

[3] G.H.C. New, "Pulse evolution in mode-locked quasi-continuous lasers", IEEE J. of Quantum Electron., **10**, 115-124 (1974).

[4] H.A. Haus, C.V. Shank, and E.P. Ippen, "Shape of passively mode-locked laser pulses", Opt. Commun., **15**, 29-31 (1975).

[5] H.Haus, "Theory of mode locking with a fast saturable absorber", J. Appl. Phys. **46**, 3049-3058 (1975).

[6] H.Haus, "Modelocking of semiconductor laser diodes", Jap. J. Appl. Phys. **20**, 1007-1020 (1981).

[7] O. E. Martinez, R. L. Fork, and J. P. Gordon, "Theory of passively mode-locked lasers including self-phase modulation and group-velocity dispersion", Opt. Lett., **9**, 156-158 (1984) .

[8] O. E. Martinez, R. L. Fork, and J. P. Gordon, "Theory of passively mode-locked lasers for the case of a nonlinear complex-propagation coefficient", J. Opt. Soc. Am. **B2**, 753-760, (1985).

[9] H.A. Haus, J.G. Fujimoto, and E.P. Ippen, "Structures for additive mode locking", J. Opt. Soc. Am. **B8**, 2068-2076 (1991).

[10] J. A. Leegwater, "Theory of mode-locked semiconductor lasers", IEEE Journal of Quantum Electron., **QE-32**, 1782-1790 (1996).

[11] R.G.M.P. Koumans and R. van Roijen , "Theory of passive mode-locking in semiconductor laser structures including the effects of self-phase modulation, dispersion, and pulse collisions", IEEE Journal of Quantum Electronics, **QE-32**, 478-492 (1996).

[12] F.X. Kärtner, I.D. Jung, and U. Keller, "Soliton mode-locking with saturable absorbers", IEEE Journal of Selected Topics in Quantum Electronics, **2**, 540-556 (1996).

[13] J. L. A. Dubbeldam, J. A. Leegwater, and D. Lenstra, "Theory of mode-locked semiconductor lasers with finite relaxation times", Appl. Phys. Lett. **70**, 1938-1940 (1997).

[14] F.X. Kärtner, J. Aus der Au, and U. Keller, "Mode-locking with slow and fast saturable absorbers – what is the difference", IEEE Journal of Selected Topics in Quantum Electronics, **4**, 159-168 (1998).

[15] J. M. Soto-Crespo and N.N. Akhmediev, "Multisoliton regime of pulse generation by lasers passively mode locked with a slow saturable absorber", J. Opt. Soc. Am. **B16**, 674-677 (1999).

[16] M. J. Lederer, B. Luther-Davies, H.H. Tan C. Jagadish, J. M. Soto-Crespo, and N.N. Akhmediev, "Multisoliton regime of pulse generation by lasers passively mode locked with a slow saturable absorber", J. Opt. Soc. Am. **B16**, 895-904 (1999).

[17] H.Haus, "Modelocking of lasers", IEEE J. of Sel. Topics in Quantum Electronics, **6**, 1173-1185 (2000).

[18] E.A. Avrutin, J.H. Marsh, and E.L. Portnoi, "Monolithic and multi-GigaHerz mode-locked semiconductor lasers: constructions, experiments, models, and applications", IEE Proc.-Optoelectron. **147**, 251 (2000).

[19] T. Kolokolnikov, T. Erneux, N. Joly, and S. Bielawski, "The Q-switching instability in passively mode-locked lasers", submitted for publication, 2004.

[20] R. Paschotta and U. Keller, "Passive mode locking with slow saturable absorbers", Appl. Phys. **B73**, 653-662 (2001).

[21] B. Tromborg, H.E. Lassen, H. Olesen, "Travelling wave analysis of semiconductor lasers", IEEE J. of Quantum Electron., **30**, 939-956 (1994).

[22] U. Bandelow, M. Radziunas, J. Sieber, M. Wolfrum, "Impact of Gain Dispersion on the Spatio-Temporal Dynamics of Multisection Lasers ", IEEE J. Quantum Electron. **37**, 183-188, (2001).

[23] G. P. Agrawal, N. A. Olsson, "Self-phase modulation and spectral broadening of optical pulses in semiconductor laser amplifiers", IEEE J. of Quantum Electron., **25**, 2997-2306 (1989).

[24] V. B. Khalfin, J. M. Arnold, and J. H. Marsh, "A theoretical model of synchronization of a mode-locked semiconductor laser with an external pulse stream", IEEE. J. Sel. Topics in Quantum Electronics, **1**, 523-527 (1995).

[25] K. Ikeda, "Multiple-valued stationary state and its instability of the transmitted light by a ring cavity", Opt. Commun., **30**, 257-261, (1979).

[26] K. Ikeda, H. Daido and O. Akomoto, "Optical turbulence: Chaotic behavior of transmitted light from a ring cavity", Phys. Rev. Lett., **45**, 709-712, (1980).

[27] N. Guglielmi and E. Hairer, Users' guide for the code RADAR5, Technical report, 2000.

[28] K. Engelborghs, T. Luzyanina, and G. Samaey, DDE-BIFTOOL v. 2.00: a Matlab package for bifurcation analysis of delay differential equations. Technical Report TW-330, Department of Computer Science, K.U.Leuven, Leuven, Belgium, 2001.

[29] E.F. Mischenko and N.Kh. Rozov, Differential equations with small parameters and relaxation oscillations, Plenum Press, New York and London (1980).

[30] T. Erneux, "Q-Switching bifurcation in a laser with a saturable absorber", J. Opt. Soc. Am. B **5**, 1063-1069 (1988).

[31] C. Hönniger, R. Paschotta, F. Morier-Genoud, M. Moser, and U. Keller, "Q-switching stability limits of continuous-wave passive mode locking", J. Opt. Soc. Am., **B16**, 46-56 (1999).

[32] J. Palaski and K.Y. Lau, "Parameter ranges for ultrahigh frequency mode locking of semiconductor lasers", Appl. Phys. Lett. **59**, 7-9 (1991).

[33] S. Yu, T. F. Krauss, P. J. R. Laybourn, "Mode locking in large monolithic semiconductor ring lasers", Opt. Eng. **37**, 1164-1168 (1991).

[34] J. P. Hohimer and G. A. Vawter, "Passive mode-locking of monolithic semiconductor ring lasers at 86 GHz", Appl. Phys. Lett. **63**, 1598-1600 (1993).

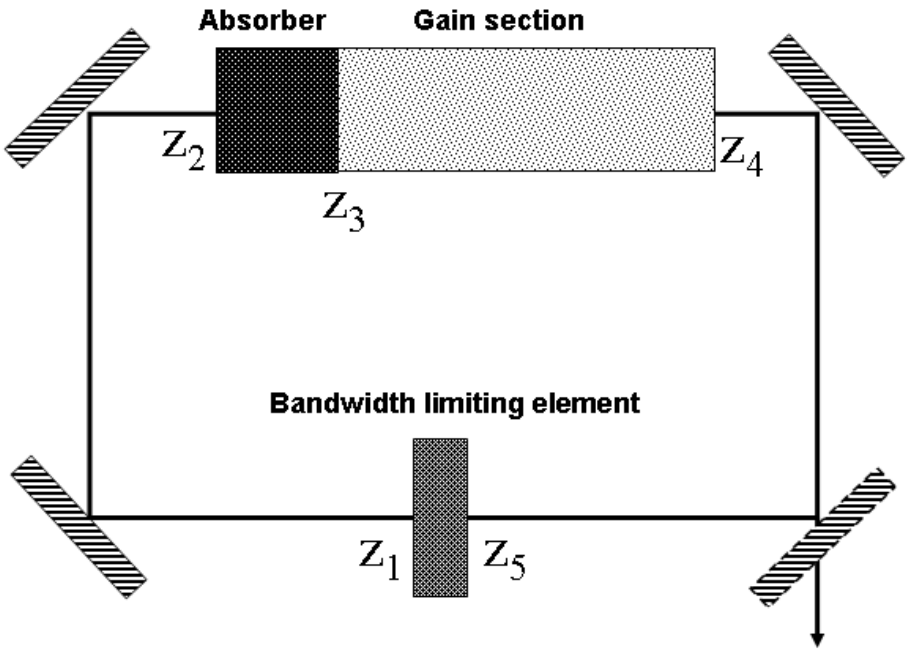

Figure 1: Schematic representation of a ring passively mode-locked laser. The coordinate z is measured along the cavity axis. The interval $z_2 < z < z_3$ ($z_3 < z < z_4$) corresponds to amplifying (absorbing) section. Spectral filtering element is placed between $z = z_5$ and $z = z_1 + L$, where L is the cavity length. The intervals $z_1 < z < z_2$ and $z_4 < z < z_5$ are filled with passive medium.

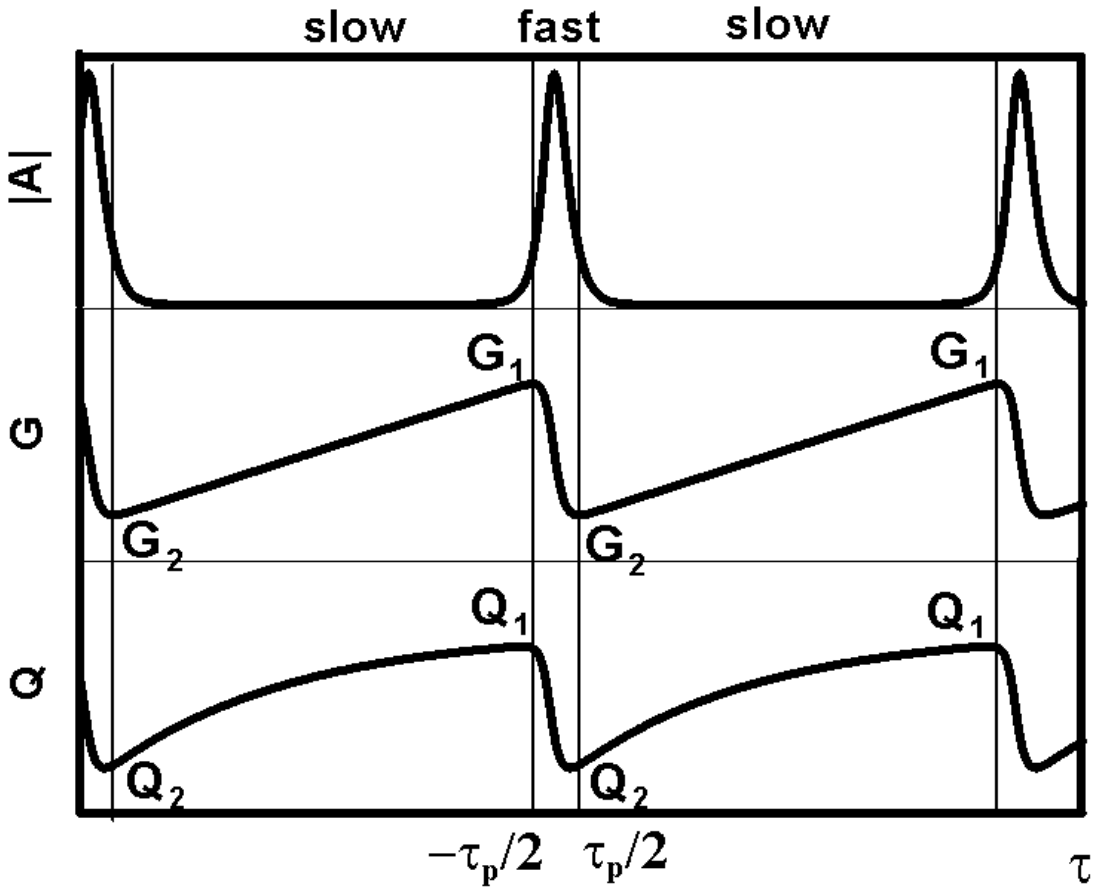

Figure 2: Time evolution of electric field intensity $|A|^2$, saturable gain G, and saturable loss Q in a laser with slow absorber. The duration of the fast stage coincides with the pulse width τ_p. G_1 and Q_1 (G_2 and Q_2) are the saturable gain and loss evaluated at the beginning (end) of the fast stage which corresponds to the end (beginning) of the slow stage.

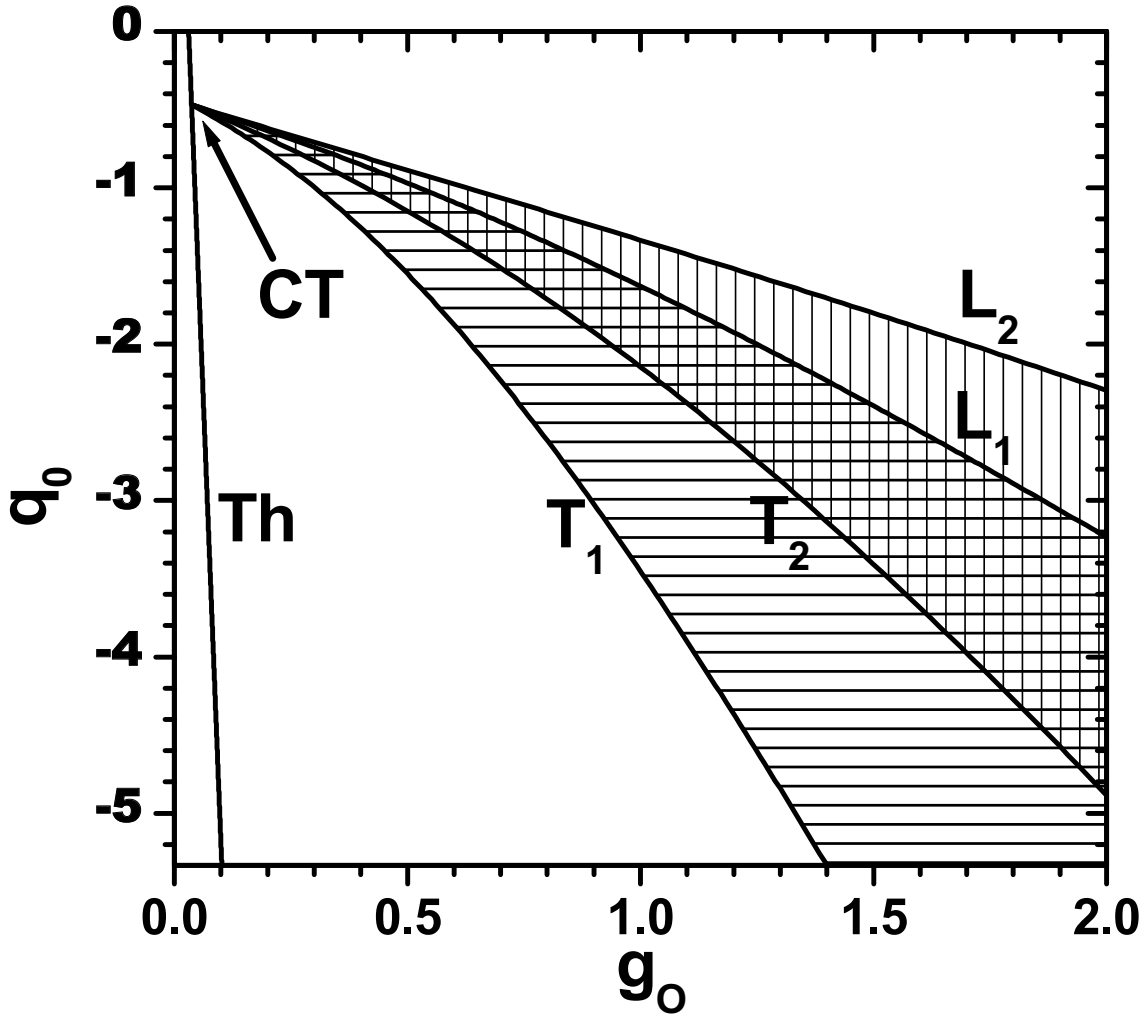

Figure 3: Background stability domains calculated using the generalization of the New's approach described in section 2.3. Horizontally (vertically) hatched area presents the background stability domain for a fundamental ML regime (a regime with twice higher repetition rate). Straight line Th corresponds to the lasing threshold. The curves $L_{1,2}$ and $T_{1,2}$ indicate the leading and trailing edge instability boundaries, respectively. CT is the codimension two point defined by Eqs. (40). The parameters are: $T = 2.5$,$s = 25$, $\Gamma = 1.33 \cdot 10^{-2}$, $\kappa = 0.1$, $\alpha_{g,q} = 0$, $\phi = 0$.

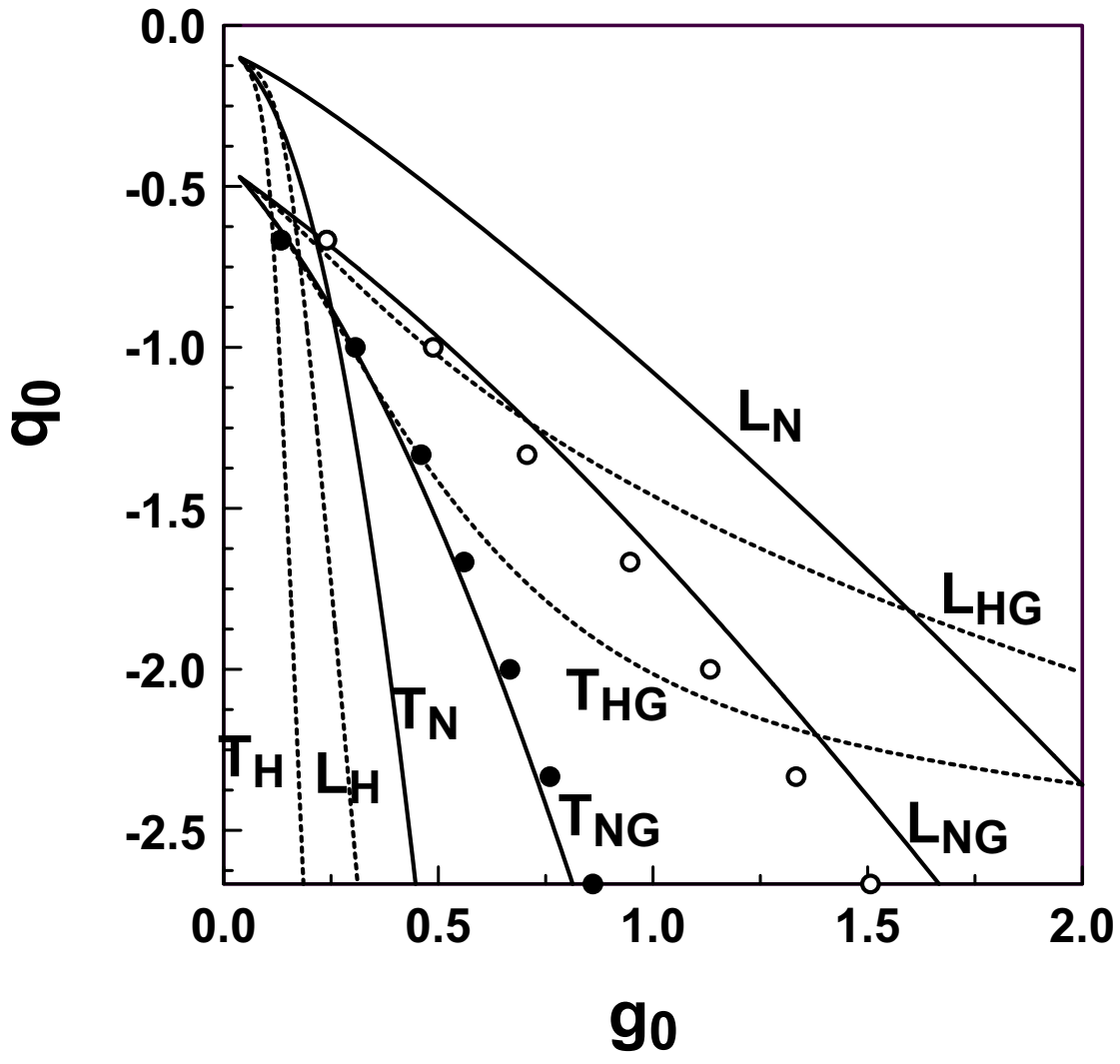

Figure 4: ML pulse background stability boundaries calculated using four different sets of equations. Solid lines L_N and T_N (l_N and t_N) indicate the leading and trailing edge instability boundaries obtained using the generalized (original) New's model. Dotted lines L_H and T_H (l_H and t_H) indicate the leading and trailing edge instability boundaries obtained using the generalized (original) Haus' model. Filled (empty) dots indicate leading (trailing) edge instability boundary calculated by numerical integration of Eqs. (24)-(26). Parameters are the same as in Fig. 3.

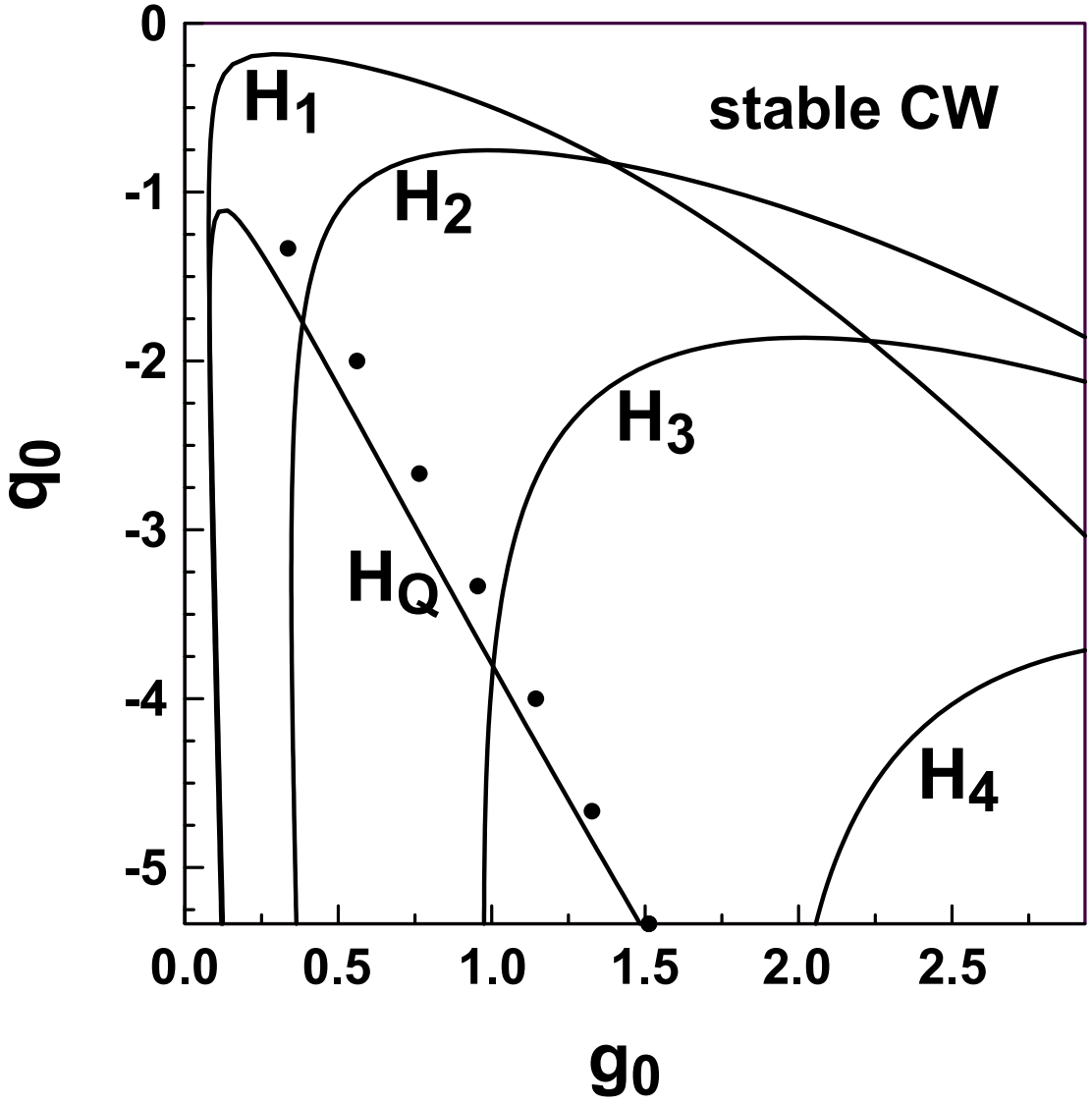

Figure 5: Hopf bifurcations of the CW solution of Eqs. (24)-(26). Curves H_n indicate Hopf bifurcations with the frequency $\Omega_n \approx 2\pi n/T$ $(n = 1, 2, 3, 4)$. Curve T_Q corresponds to a Hopf bifurcation with the frequency approximately one order of magnitude smaller than $2\pi/T$ (Q-switching frequency). Black dots indicate a Q-switching instability boundary of a fundamental ML regime. $\gamma = 33.3$. Other parameters are the same as in Fig. 3.

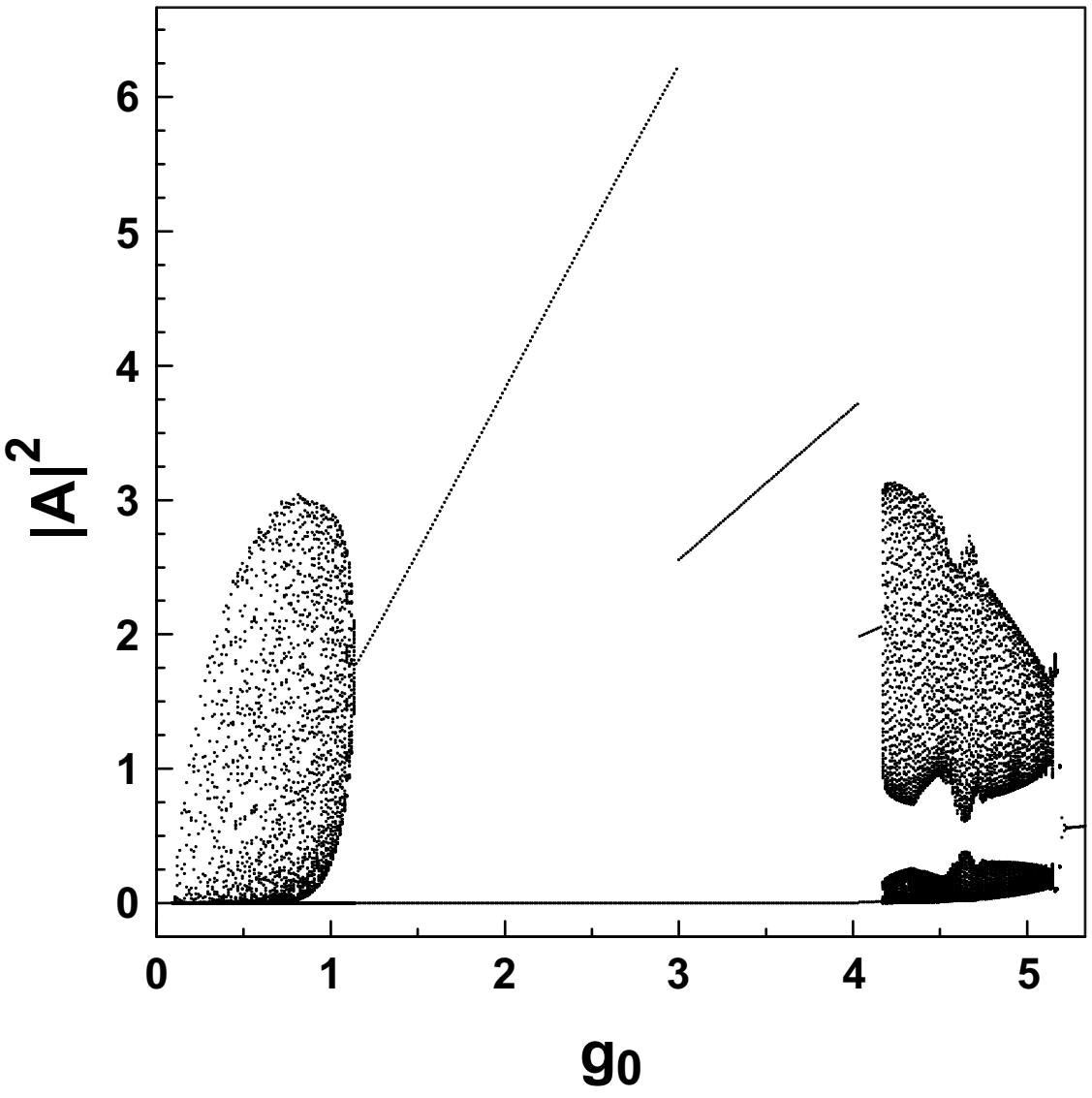

Figure 6: Bifurcation diagram obtained by direct numerical simulation of Eqs. (24)-(26) with $q_0 = 3$. Other parameters are the same as in Fig. 5.

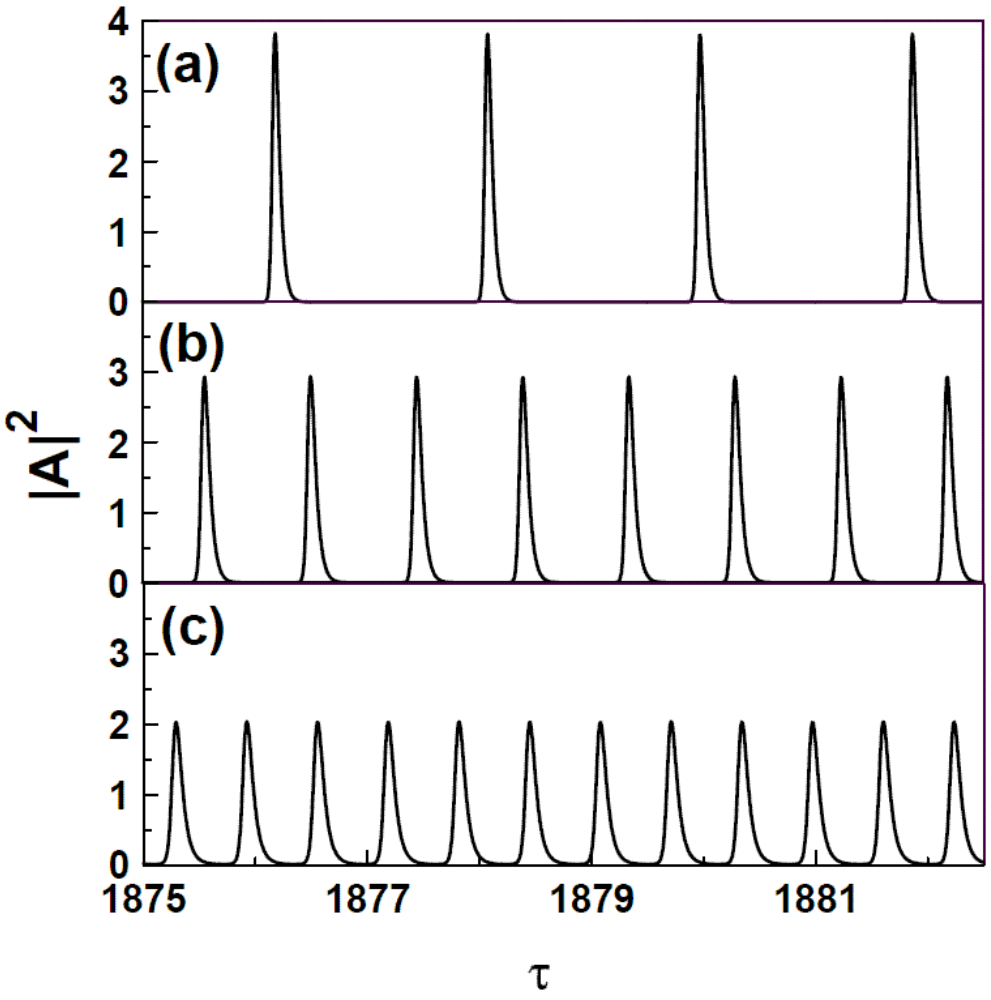

Figure 7: Periodic intensity time traces corresponding to different ML regimes. (a) Fundamental ML regime, $g_0 = 2.0$; (b) ML regime with two pulses in the cavity, $g_0 = 3.33$; (c) ML regime with three pulses in the cavity, $g_0 = 4.13$. Other parameters are the same as in Fig. 6.

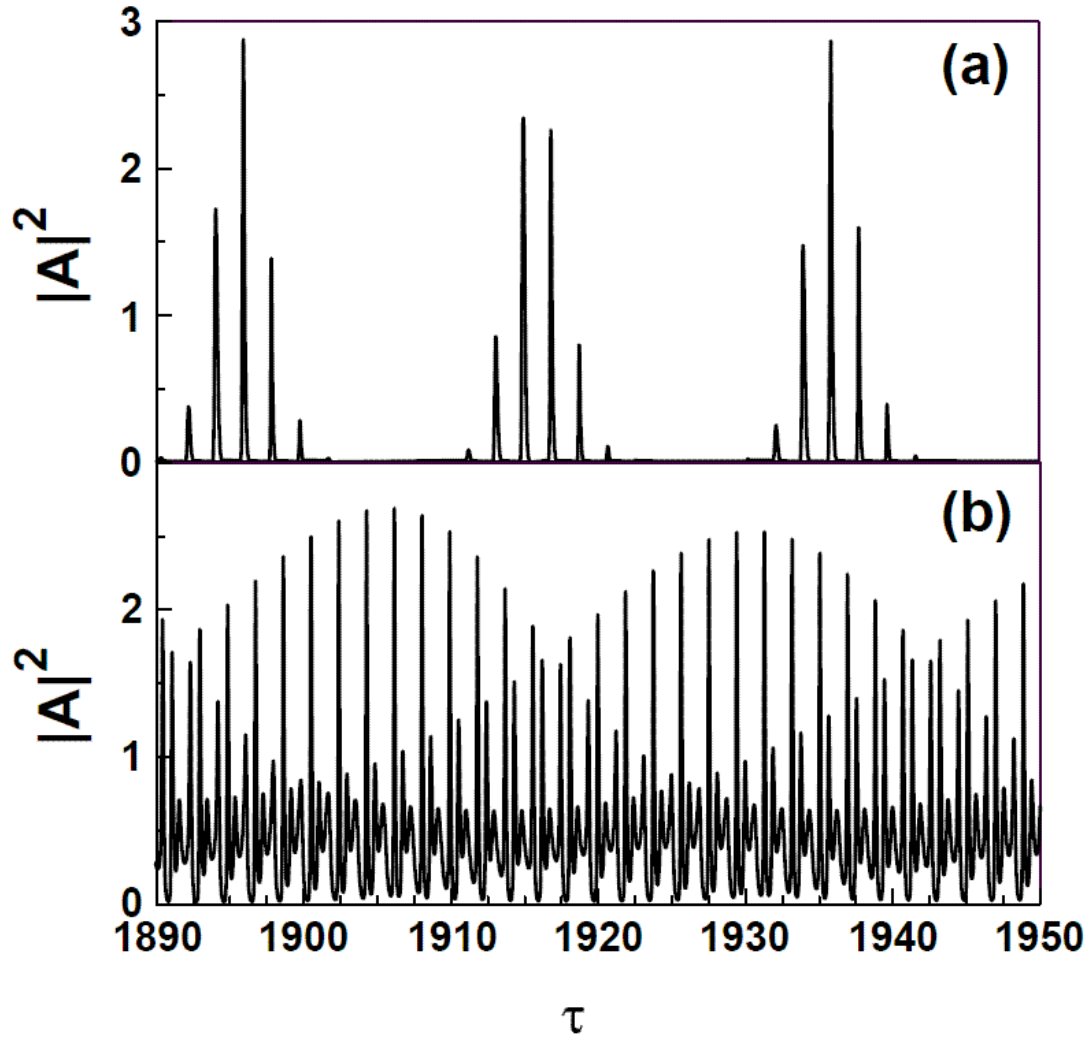

Figure 8: Nonperiodic intensity timetraces. (a) ML solution modulated by Q-switching frequency, $g = 0.67$; (b) a regime that appears after the break-up of the periodic ML regime shown in Fig. 7c, $g = 4.67$. Other parameters are the same as in Fig. 6.

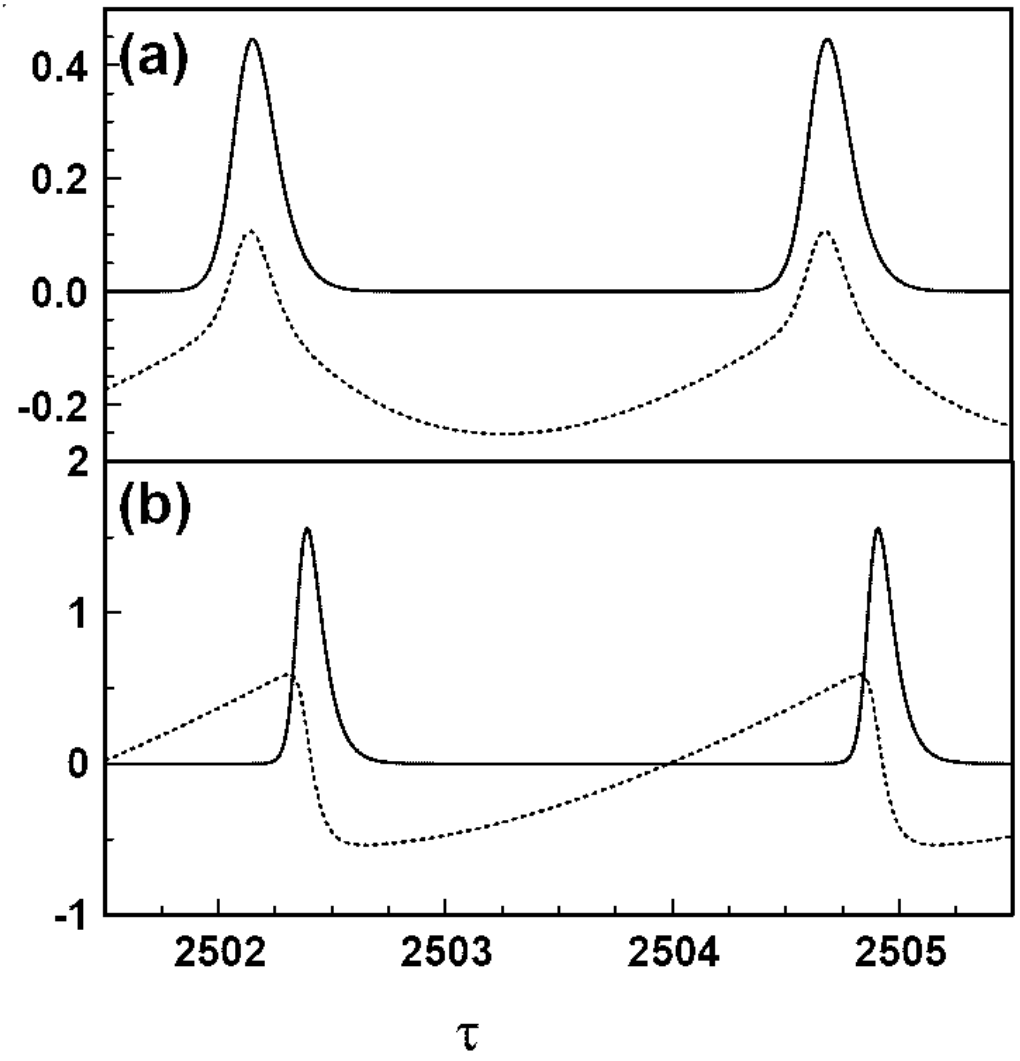

Figure 9: Time dependency of the laser intensity (solid line) and the net gain parameter (dotted line). (a) ML pulses with "stable" background, $g_0 = 0.6$; (b) ML pulses with "unstable" background at the leading edge, $g_0 = 1.33$. $q_0 = 1.33$. Other parameters are the same as in Fig. 5.

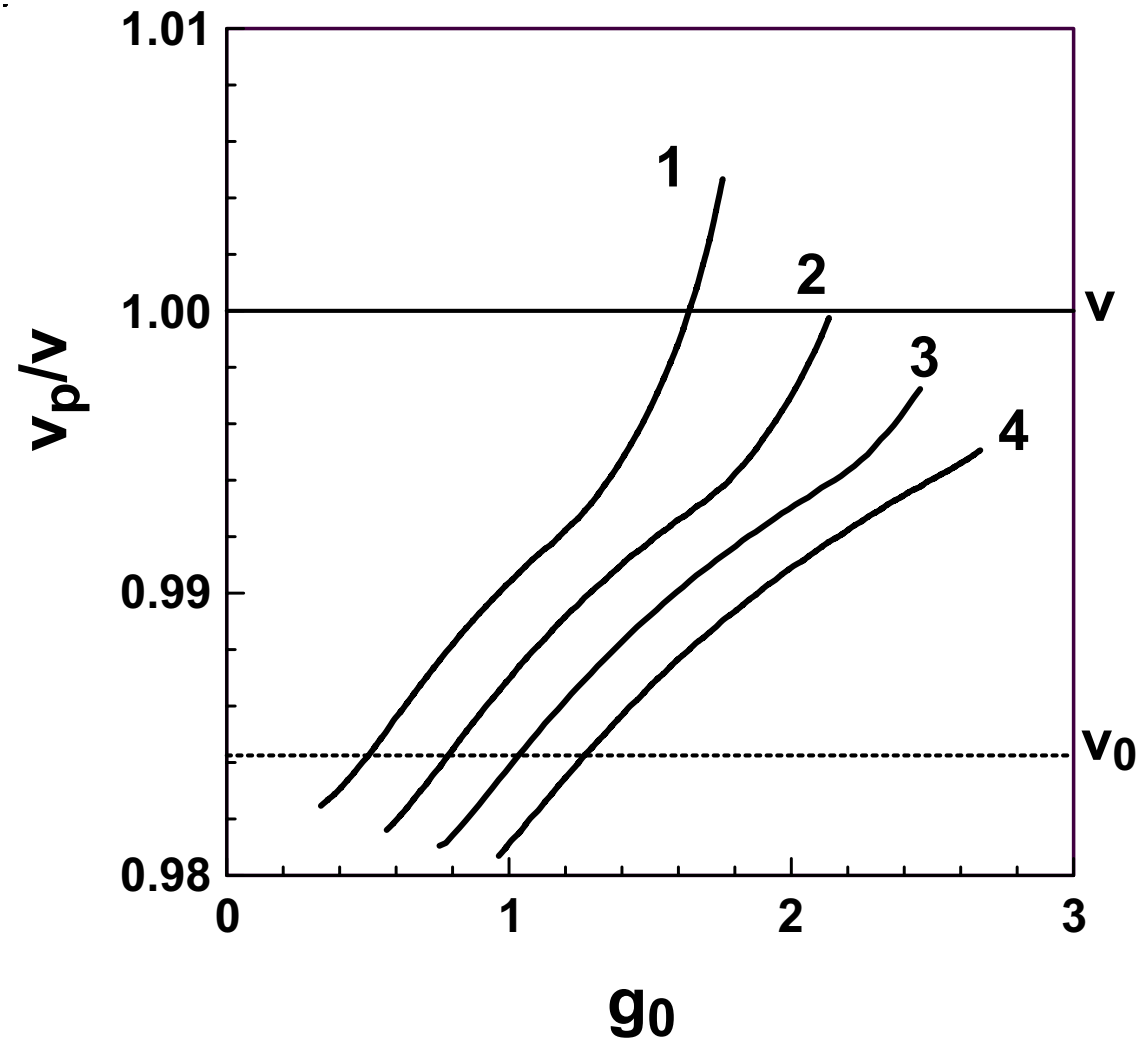

Figure 10: Normalized repetition frequency of a fundamental ML regime vs pump parameter. 1 - $q_0 = 1.33$, 2 - $q_0 = 2.0$, 3 - $q_0 = 2.67$, 4 - $q_0 = 3.33$. Other parameters are the same as in Fig. 5.

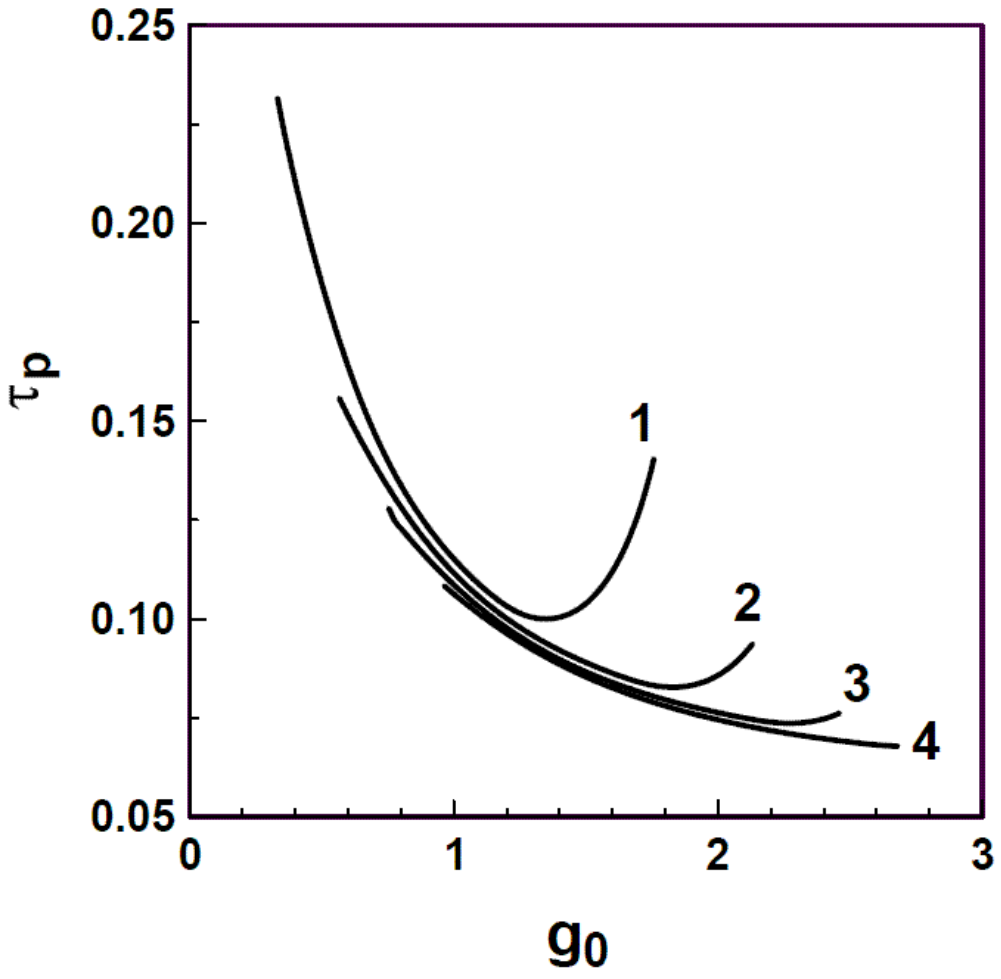

Figure 11: Normalized pulse width of a fundamental ML regime vs pump parameter. 1 - $q_0 = 1.33$, 2 - $q_0 = 2.0$, 3 - $q_0 = 2.67$, 4 - $q_0 = 3.33$. Other parameters are the same as in Fig. 5.